Chapter 2

Phase noise and timing jitter of harmonic mode-locked and injection-locked erbium-doped fiber lasers

2.1 Introduction

Typically, the harmonic mode-locking (HML) and the injection-locking (IL) are two principle techniques used in erbium-doped fiber laser (EDFL) systems for generating ultrashort and high repetition-rate optical pulse-train [2.1, 2.2], which is mandatory for applications in high-speed optical time division multiplexed (OTDM) transmission system [2.3] and electro-optical sampling systems [2.4]. In principle, the harmonic mode-locked EDFL can be implemented by using a Mach-Zehnder intensity modulator (MZM) [2.1, 2.2] or a semiconductor optical amplifier (SOA) based loss modulator [2.5], whereas the injection-locked EDFL can simply be constructed by seeding the EDFL with a gain-switched laser diode (GSLD) [2.6]. In particular, Li. *et al.* use the FPLD as alternative intensity modulation and a mode-locker to achieve injection-locking [2.6]. Such an injection-locking was reported to exhibit extremely low phase noises, small timing jitters and supermode-noise-free output performances [2.7].

In contrast, most of the HML-EDFLs are sensitive to environmental perturbations such as temperature fluctuations and mechanical vibrations due to their relatively long cavity length associated with and numerous longitudinal modes. Thus, the HML-EDFLs pulses usually suffers from both the single-sided-band (SSB) phase noise

and the supermode noise (SMN). In most applications, the phase noise induced pulse-to-pulse timing jitter seriously degrades temporal resolution or the bit error rate (BER) performances [2.8]. To overcome, a regeneratively mode-locked EDFL was demonstrated to suppress supermode noise and the SSB phase noise (as well as timing jitter) [2.9-2.11]. Later on, Duan. *et al*. reported that the SMN and intensity noises in pulses can be greatly suppressed by adding an SOA as a high-pass filter [2.12]. In addition, Schell *et al.* reported the reduction of SSB phase noise and timing jitter in GSLD with self-feedback injection [2.13].

2.2 Experimental Setup

Figure 2.1 illustrates a typical HML-EDFL with an intra-cavity MZM based mode-locker, which consists of an erbium-doped fiber amplifier (EDFA), a pair of Faraday optical isolators, a polarization controller (PC), a $LiNbO_3$ MZM and an optical coupler (OC) with 10 % output coupling ratio. The MZM is biased at its half-wave voltage ($V_\pi \cong$ 8 V) and is driven by a microwave synthesizer with power of 22 dBm at 997.15 MHz. The PC is properly adjusted to optimize the polarization orientation of the circulating pulses which input to the MZM, and a pair of Faraday optical isolators ensures the unidirectional propagation of light in EDFL cavity. A stable HML-EDFL pulse-train can be obtained when the modulation frequency is detuned to coincide with one harmonic of longitudinal modes in the EDFL cavity.

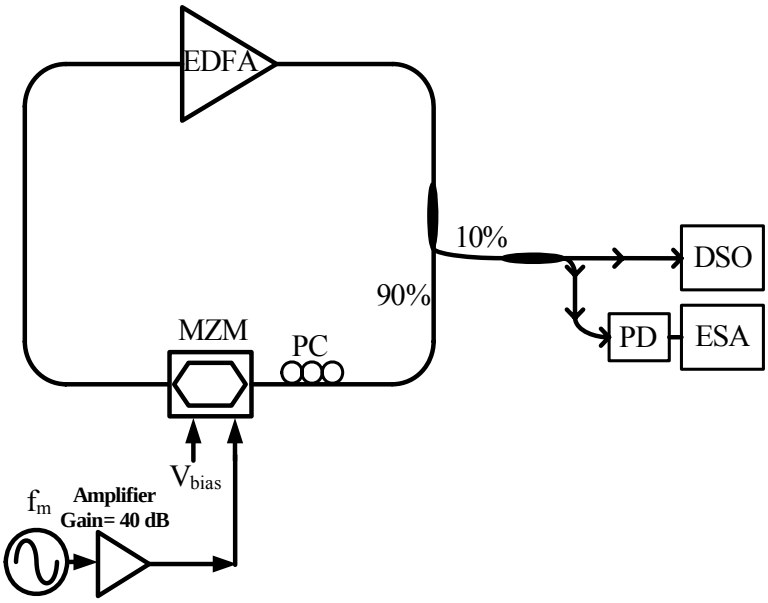

Fig. 2.1 The schematic diagram of the HML-EDFL. The V_{bias} is set at 8 V for linear operation. PC: polarization controller; OC: optical coupler; EDFA: erbium-doped fiber amplifier; and MZM: Mach-Zehnder intensity modulator

The GSLD-IL-EDFL for parametric comparison is performed by seeding the EDFL with a gain-switched Fabry–Perot laser diode (FPLD), as shown in Fig. 2.2. It consists of a comb generator, a FPLD, an EDFA, an optical circulator, a pair of Faraday optical isolators, an OBPF, and an OC of 10 % output coupling ratio. The wavelength, threshold current, and longitudinal mode spacing of the free-running FPLD operated at 25 ^{o}C are about 1550 nm, 8 mA and 1.2 nm, respectively. A comb generator driven by 27-dBm microwave signal at 1 GHz is employed to provide an electrical pulse-train for gain-switching the FPLD which is dc-baised at 3.4 mA. The central wavelength of the OBPF is adjusted to match that of the FPLD (at 1550nm), which helps to filter out the amplified spontaneous emission (ASE) of the EDFL. In particular, the amplified GSLD pulse from EDFL is feedback injected into the FPLD, achieving mutual injection-locking between the GSLD-EDFL link. Such a configuration effectively suppresses the ASE as well as the SSB phase noise of the EDFL. The feedback injection from EDFL is also used to facilitate single

longitudinal mode lasing of FPLD with improved supermode noise-suppression ratio (SMSR). Note that the feedback wavelength of the EDFL amplified GSLD pulses must coincide with the central longitudinal mode of the FPLD at 1550 nm in order to obtain the lowest SSB phase noise (timing jitter) and highest SMSR.

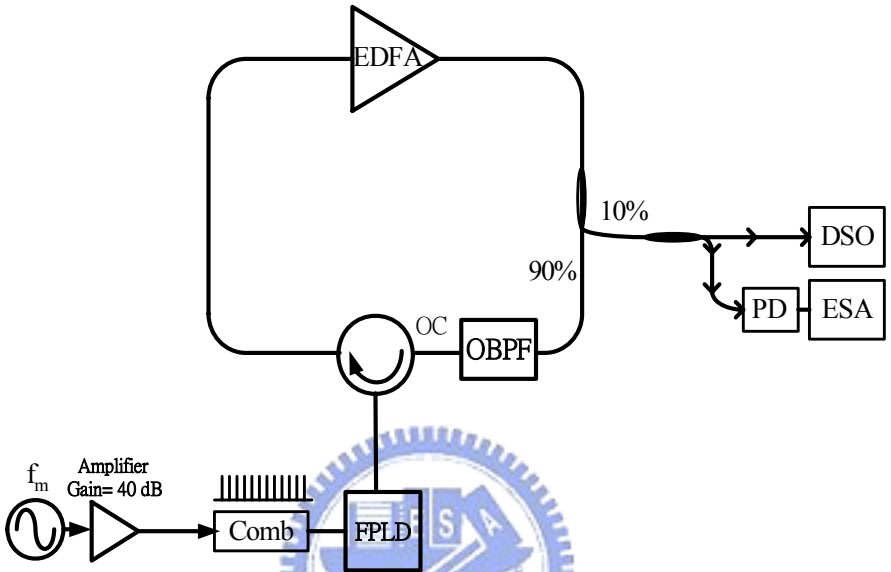

Fig. 2.2 The schematic diagram of the injection-locking by seeding the EDFL with a gain-switched Fabry –Perot laser diode (GSLD). Comb: Electrical pulse generator; EDFA: Erbium-doped fiber amplifier; OC: Optical coupler; OBPF: Optical band-pass filter; FPLD: Fabry-Perot laser diode

The pulsewidth and output power are monitored using a digital sampling oscilloscope (Agilent, 86100A+86109B), an optical spectrum analyzer with 0.01-nm resolution (Advantest, Q8384) and an optical power meter (ILX Lightwave, OMM-6810B+6727B), respectively. Assuming that the optical pulse-train exhibit small and stationary phase deviations (i.e., small timing jitter) without any secondary phase deviating sidebands, a spectral domain technique is employed to characterize the SSB phase noise and pulse-to-pulse timing jitter characteristics of the EDFL pulses [2.14, 2.15-2.19]. Such technique neglects the influences of pulse shape and pulsewidth fluctuations, which assumes no correlation between

amplitude and phase fluctuations. The SSB phase noise is quantified by measuring the noise spectral power density with an electrical spectrum analyzer (ESA, Agilent HP8565E) at a resolution bandwidth of 1 Hz in connection with a photodetector (New Focus 1014). The timing jitter and the SMSR in a given bandwidth are then calculated and analyzed from the RF spectrum using a phase-noise-utility software. By subtracting the SSB phase noise spectrum at a higher harmonic frequency (for example, the 10th harmonics, n = 10) with that at the fundamental frequency (n = 1) of the EDFL pulses, the rms timing jitter in a bandwidth extending from f_L to f_H is given by [2.20]:

$$\sigma(f) = \frac{1}{2\pi f_0}\left\{2\int_{f_L}^{f_H}\left[\left(\left[10^{L_n(f)/10} - 10^{L_1(f)/10}\right]\right)/\left(n^2-1\right)\right]df\right\}^{1/2}$$

where f_L and f_H are integration boundaries, $L_1(f)$ and $L_n(f)$ are phase noise power spectral densities of fundamental and n^{th} harmonics signals, respectively. The n denotes the harmonic number and f_0 is the repetition frequency of the laser pulse.

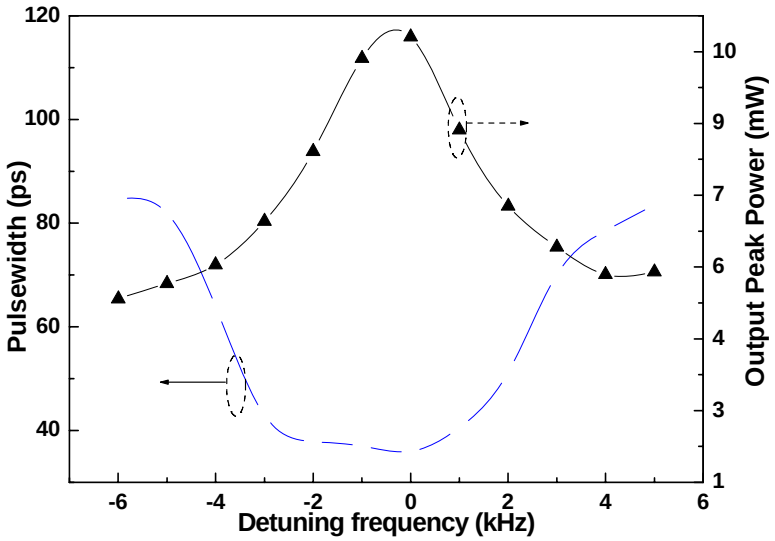

Fig. 2.3 The peak power (▲ dash line) and pulsewidth (■ solid line) variation as the driving frequency is detuned in the HML-EDFL configuration. The peak power pulsewidth at zero detuning frequency are 10.8 mW and 36 ps, respectively.

2.3 Results and Discussion

In experiment, the optimized mode-locking of HML-EDFL is determined from the evolution of pulse shape, especially the observation on the maximum peak power and the shortest pulsewidth versus detuning frequency, as shown in Fig. 2.3. It is clearly observed that the degradation on the peak power and the broadening of the pulse become more serious as the frequency is positive-detuned. The 3-dB detuning bandwidth (defined as the doubling in pulsewidth as compared to that at optimized mode-locking) of the HML-EDFL is only 7 kHz. At optimal condition, the configuration generated the shortest pulsewidth of 36 ps and maximum output peak power of 12.3 mW, respectively, as shown in Fig. 2.3. In conventional HML-EDFL, the SSB phase noises and timing jitter at offset frequency of 100 kHz are -114 dBc/Hz and 0.6 ps, respectively, as shown in Figs. 2.4 and 2.5.

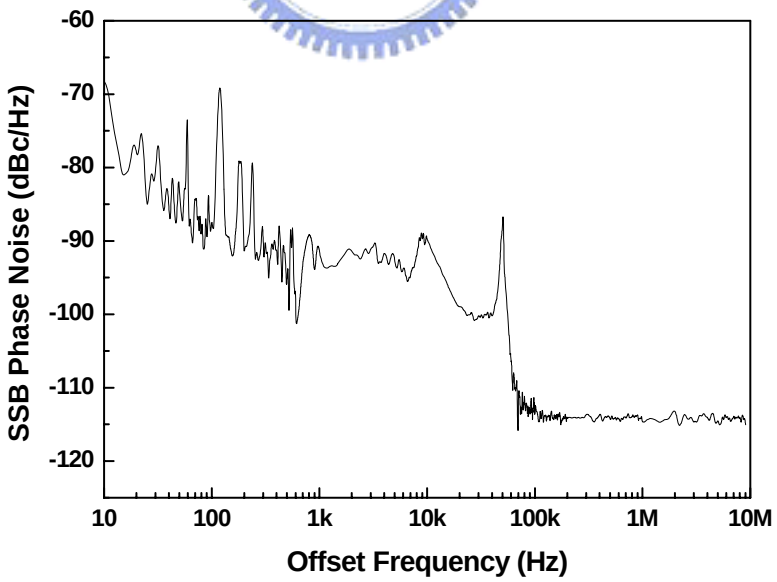

Fig. 2.4 The SSB phase noise in HML-EDFL.

The low-frequency spurs are mainly due to the 60-Hz wall current and its

harmonics. The other vibration spurs at harmonics of 20 and 55 Hz that are due to ac fans and other ambient vibrations [2.21]. It is found that the SMN suppression ratio is only 45 dB. Note that supermode noise is generated as a result of beating between the lasing mode and amplified spontaneous emission and causes large fluctuations in the intensity of the laser output. Typically, the extremely long upper-level lifetime of excited erbium ions in EDFL (~10 ms) may lead to a large power fluctuation and a strong supermode beating effect of the output pulse.

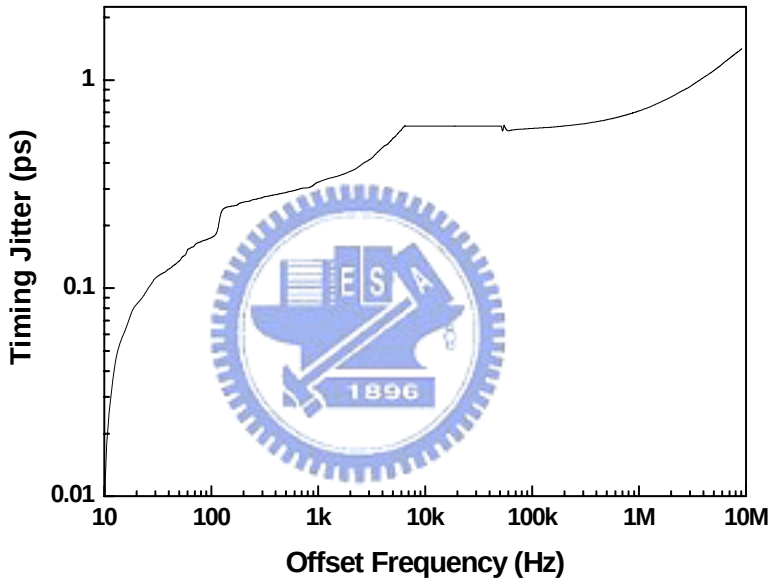

Fig. 2.5 The timing jitter in HML-EDFL.

In comparison, the GSLD pulse experiences a resonant amplification process in the EDFL. In such a GSLD-IL-EDFL, the GSLD injected pulse reaches its highest peak power and shortest pulsewidth as the repetition frequency coincides with the harmonic frequency of the longitudinal mode in EDFL. Otherwise, the repetition frequency mismatch with the harmonic mode frequency of the resonant EDFL cavity. When the repetition frequency detunes, the pulses circulated in the EDFL arrives the gain medium with a slight temporal deviation, this eventually leads to a broadened

pulse shape which is contributed by the superpositioned pulses. The 3-dB detuning bandwidth of GSLD-EDFL is 17.78 kHz (see Fig. 2.6). The multi-pulse effect appears as the gain-switching frequency detunes beyond this bandwidth. In such a GSLD-IL-EDFL link, the output power and pulsewidth versus frequency detuning are shown in Fig. 2.6.

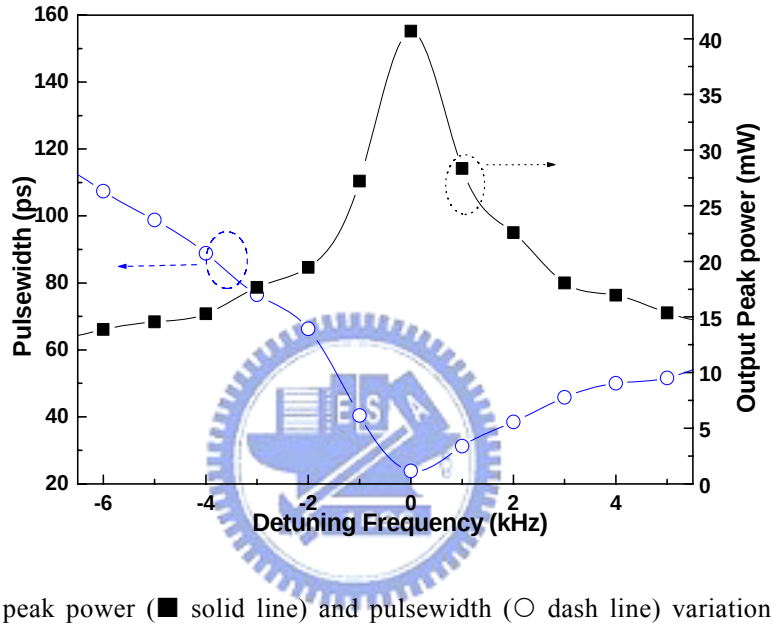

Fig. 2.6 The peak power (■ solid line) and pulsewidth (○ dash line) variation as the driving frequency is detuned in GSLD-EDFL configuration. The peak power pulsewidth at zero detuning frequency are 40.7 mW and 22 ps, respectively.

At optimal condition, the peak power of 40.7 mW and the pulsewidth of 22 ps are obtained, and the injection-locked pulse shape is shown in Fig. 2.7. The SSB phase noise and corresponding timing jitter of a free-running GSLD free-running are -113.7 dBc/Hz at 100 kHz offset frequency and 0.32 ps between a frequency interval of 10 Hz and 100 kHz, respectively, as illustrated in Figs. 2.8(a) and 2.9(a). However, the GSLD-EDFL (with feedback injection) has lower phase noise of -121.2 dBc/Hz and timing jitter of 0.25 ps than those of a free-running GSLD, as shown in Figs. 2.8(b) and 2.9(b).

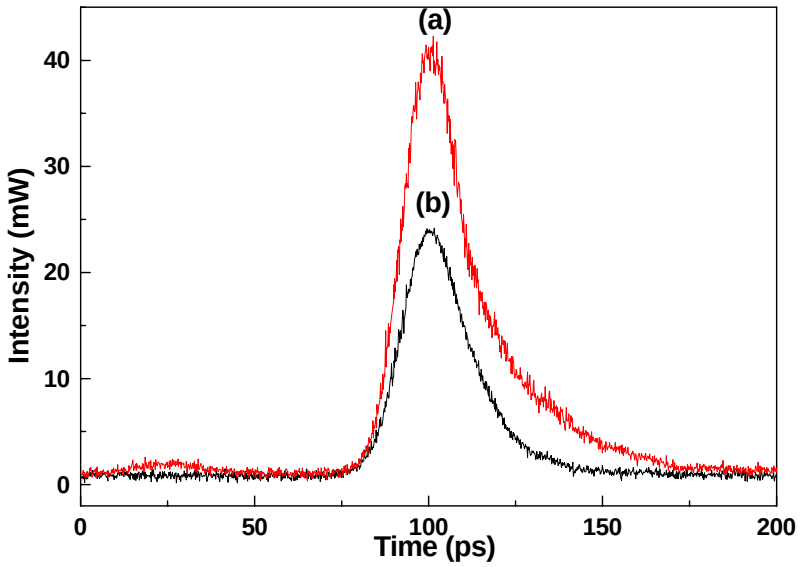

Fig. 2.7 The pulsewidth under optimal operating condition. (a) the peak power of the GSLD free-running (without feedback injection) is 23.8 mW (b) the peak power of the GSLD-EDFL (with feedback injection) is 40.7 mW.

This is due to the reduction in spontaneous emission noise of the GSLD under such a mutually injection-locked GSLD-IL-EDFL link. Furthermore, the SMN suppression ratio of the GSLD-IL-EDFL system is also enhanced from 87 to 91 dB, as shown in Fig. 2.10. Such an excellent supermode noise suppression is caused by the intensity-dependent gain of the FPLD, which tends to equalize the pulse energies as a result of gain saturation [2.7]. Note that the FPLD based filtering effect is due to its relatively fast carrier recovery rate (from 0.5 to 1 ns) and gain saturation effect. In comparison, the SMN suppression ratio and SSB phase noise (timing jitter) of the GSLD-IL-EDFL are far better than those of the HML-EDFL.

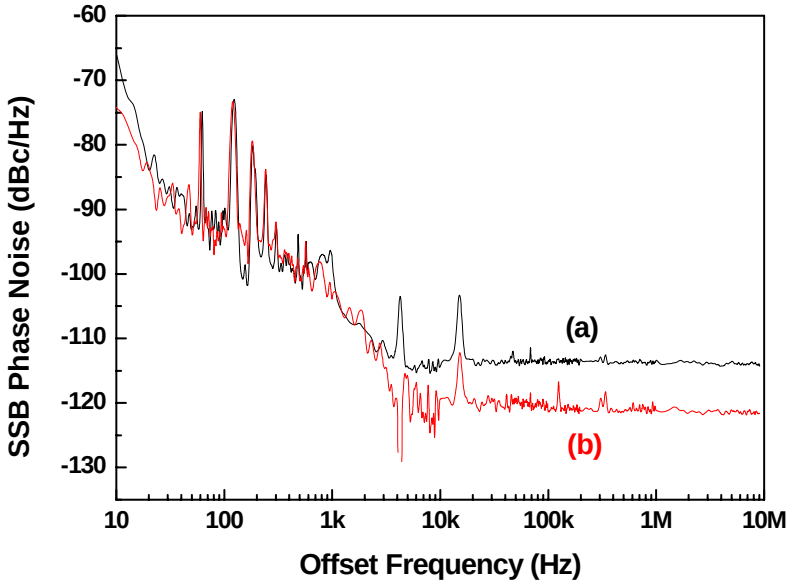

Fig. 2.8 The SSB phase noise in GSLD (a) without feedback injection and (b) with feedback injection (*i.e.* GSLD-IL-EDFL).

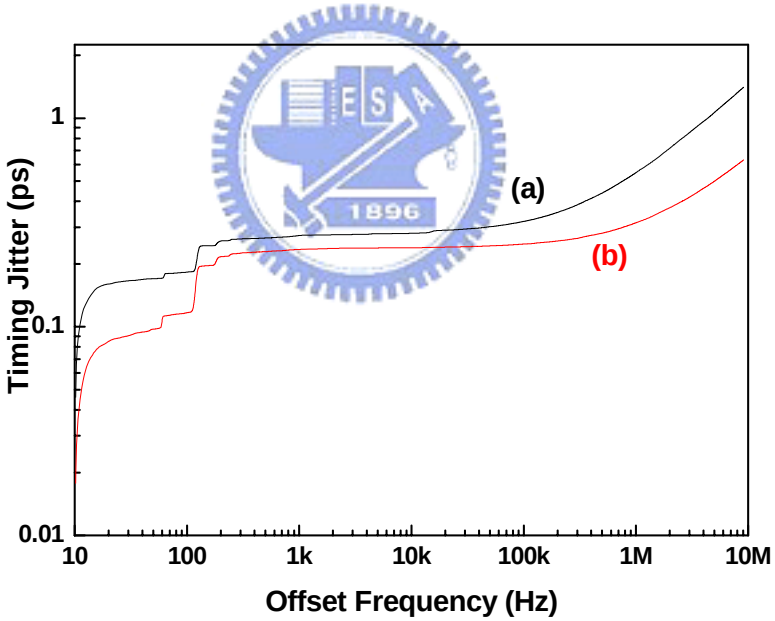

Fig. 2.9 The timing jitter in GSLD (a) without feedback injection and (b) with feedback injection.

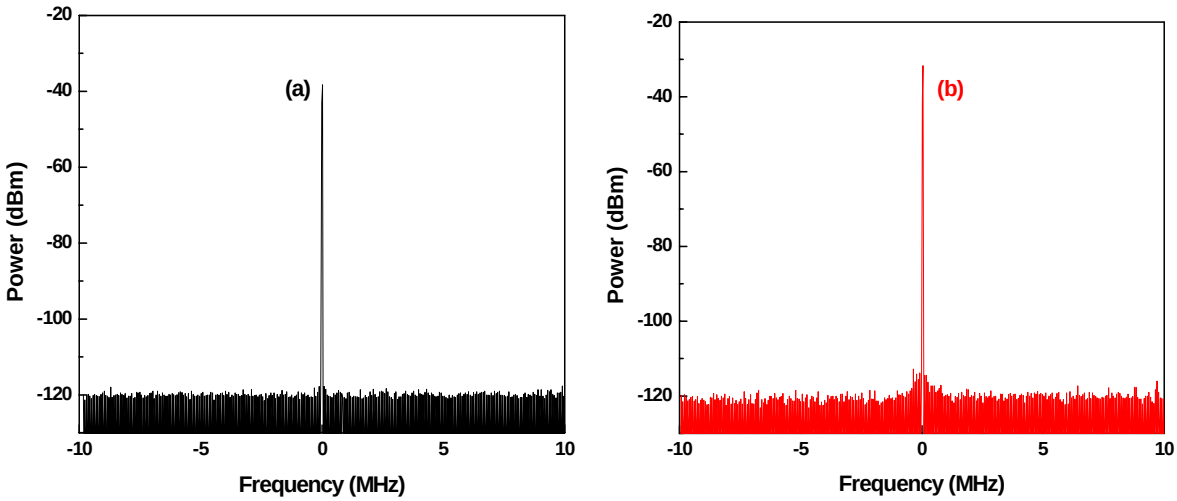

Fig. 2.10 The supermode noise in GSLD (a) without feedback injection and (b) with feedback injection (VBW=10 Hz; RBW=10 Hz; and SPAN=20 MHz).

2.4 Conclusion

In conclusion, we compare the noise properties of the HML-EDFL and GSLD-EDFL, including SSB phase noise, timing jitter, SMN. In addition, we also compare the 3-dB detuning bandwidth of the HML-EDFL and GSLD-EDFL. The comparisons between HML- and GSLD-EDFL are demonstrated that the GSLD-EDFL exhibits better performances than HML-EDFL. The 3-dB detuning bandwidth of 17.78 kHz in GSLD-EDFL has 2.54 times larger than that of 7 kHz in HML-EDFL. Moreover, the high peak power of 40.7 mW and a smaller pulsewidth of 22 ps can be obtained in GSLD-EDFL. In GSLD-EDFL, the FPLD acts as a SMN suppressor due to its relatively fast carrier recovery rate (from 0.5 to 1 ns) and gain saturation effect. So the SMN is suppressed by the FPLD itself, and the SSB phase noise correlated the intensity noise can be effectively reduced. By this reason, the SSB phase noise and timing jitter of -121.2 dBc/Hz, and 0.25 ps in GSLD-EDFL are indeed lower than that of -114 dBc/Hz and 0.6 ps in HML-EDFL. Because the FPLD acts as a SMN

suppressor, the SMN suppression of 91 dB in GSLD-EDFL is higher than that of 45 dB in HML-EDFL. Furthermore, the side-mode in GSLD-EDFL can be entirely suppressed due to the effects of intra-cavity OBPF and injection-locking. Further, we add an intra-cavity SOA and OBPF to improve the SMN suppression ratio without sacrificing the SSB phase noise in HML-EDFL.

2.5 References

[2.1] K. K. Gupta and D. Novak, "Millimeter-wave repetition-rate optical pulse train generation in harmonically modelocked fiber ring laser," Electron. Letter., vol. 33, pp. 1330-1331, 1997.

[2.2] R.P. Davey, K. Smith, A. McGuire, "High-speed mode-locked, tunable, integrated erbium fibre laser," Electron. Letter., vol. 28, pp. 428-483, 1992.

[2.3] S. Kawanishi, K. Okamoto, M. Ishii, O. Kamatani, H. Takara, and K. Uchiyama, "All-optical time-division-multiplexing of 100 Gbit/s signal based on four-wave mixing in a travelling-wave semiconductor laser amplifier," Electron. Lett., vol. 33, pp. 976-977, 1997.

[2.4] S. Kawanishi, K. Okamoto, M. Ishii, O. Kamatani, H. Takara, and K. Uchiyama, "All-optical time-division-multiplexing of 100 Gbit/s signal based on four-wave mixing in a travelling-wave semiconductor laser amplifier," Electron. Lett., vol. 33, pp. 976-977, 1997.

[2.5] T. Papakyriakopoulos, K. Vlachos, A. Hatziefremidis, and H. Avramopoulos, "20-GHz broadly tunable and stable mode-locked semiconductor amplifier fiber ring laser," Opt. Lett., vol. 24, pp. 209-1211, 1999.

[2.6] Shenping Li and K. T. Chan, "Actively mode-locked erbium fiber ring laser using a Fabry–Perot semiconductor modulator as mode locker and tunable filter," Appl.

Phys. Lett., vol. 74, pp. 2737-2740, 1999.

[2.7] S. Li and K. T. Chan, “Wavelength-tunable actively mode-locked erbium-doped fiberring laser using a distributed feedback semiconductor laser as mode locker and tunable filter,” Appl. Phys. Lett., vol. 75, pp. 313-315, 1999.

[2.8] M. Jinno, “Effect of timing jitter on an optically-controlled picosecond optical switch,” Opt. Lett., vol. 18, pp. 1409-1411, 1993.

[2.9] K. K. Gupta, D. Novak, and Liu Hai-Feng, “Noise characterization of a regeneratively mode-locked fiber ring laser,” IEEE J. Quantum Electron., vol. 36, pp. 70-78, 2000.

[2.10] E. Yoshida and M. Nakazawa, “Measurement of the Timing Jitter and Pulse Energy Fluctuation of a PLL Regeneratively Mode-Locked Fiber Laser,” IEEE Photon. Technol. Lett., vol. 11, pp. 548-550, 1999.

[2.11] M. Nakazawa, E. Yoshida, and K. Tamura, “10GHz, 2ps regeneratively and harmonically FM mode-locked erbium fibre ring laser,” Electron. Lett., vol. 32, pp. 1285-1287, 1996.

[2.12] L. Duan, C. J. K. Richardson, Z. Hu, M. Dagenais, and J. Goldhar, “A stable smoothly wavelength-tunable picosecond pulse generator,” IEEE Photon. Technol. Lett., vol. 14, pp. 840-842, 2002.

[2.13] M. Schell, W. Utz, D. Huhse, J. Kassner and D. Bimberg, “Low jitter single-mode pulse generation by a self-seeded, gain-switched Fabry-Perot semiconductor laser,” Appl. Phys. Lett., vol. 65, pp. 3045-3047, 1994.

[2.14] K. K. Gupta, D. Novak, and H.-F. Liu, “Noise characterization of a regeneratively mode-locked fiber ring laser,” IEEE J. Quantum Electron. vol. vol. 36, pp. 70-78 , 2000.

[2.15] D. Von der Linde, “Characterization of the noise in continuously operating

mode-locked laser," Appl. Phys. B, vol. 39, pp. 201-217, 1986.

[2.16] M. J. W. Rodwell, D. M. Bloom, and K. J. Weingarten, "Subpicosecond laser timing stabilization," IEEE J. Quantum Electron., vol. 25, pp. 817-827, 1989.

[2.17] U. Keller, K. D. Li, M. J. W. Rodwell, and D. M. Bloom, "Noise characterization of femtosecond Raman soliton laser," IEEE J. Quantum Electron., vol. 25, pp. 280-288, 1989.

[2.18] A. Finch, X. Zhu, P. N. Kean, and W. Sibbett, "Noise characterization of mode-locked color-centre laser sources," IEEE J. Quantum Electron., vol. 26, pp. 1115-1123, 1990.

[2.19] A. J. Taylor, J. M. Wiesenfeld, G. Eisenstein, and R. S. Tucker, "Timing jitter in a mode-locked and gain-switched InGaAsP injection lasers," Appl. Phys. Lett., vol. 49, pp. 681-683, 1986.

[2.20] P. Pepeljugoski, J. Lin, J. Gamelin, M. Hong, and K. Y. Lau, "Ultralow timing jitter in electrically gain-switched vertical cavity surface emitting lasers," Appl. Phys. Lett., vol. 62, pp. 1588-1590, 1993.

[2.21] L. A. Jiang, M. E. Grein, and E. P. Ippen, "Quantum-limited noise performance of a mode-locked laser diode," Opt. Lett., vol. 27, pp. 49-51, 2002.

[2.22] T. Saitoh and T. Mukai, "1.5μm GaInAsP Traveling-Wave Semiconductor Laser Amplifier," IEEE J. Quantum Electron., vol. 23, pp. 1010-1020, 1987.